Title: Neutrophils prime unique transcriptional responses in intestinal organoids during infection with nontyphoidal *Salmonella enterica* serovars

Authors/Affiliations

Anna-Lisa E. Lawrence[1], Ryan P. Berger[1], David R. Hill[2], Sha Huang[3], Veda K. Yadagiri[2], Brooke Bons[2], Courtney Fields[2], Jason S. Knight[2], Christiane E. Wobus[1], Jason R. Spence[3], Vincent B. Young[1,2], Basel H. Abuaita[1,a,b], and Mary X. O'Riordan[1a]

[1] Department of Microbiology and Immunology, University of Michigan Medical School, Ann Arbor, MI, USA

[2] Department of Internal Medicine/Infectious Diseases Division, University of Michigan Medical School, Ann Arbor, MI, USA

[3] Department of Cell and Developmental Biology, University of Michigan Medical School, Ann Arbor, MI, USA

Author list footnotes

[a] M.X.O and B.H.A contributed equally to the work

[b] B.H.A Present address: Department of Pathobiological Sciences, Louisiana State University School of Veterinary Medicine, Baton Rouge, LA, USA

Contact Info

***Correspondence: babuaita@lsu.edu, oriordan@umich.edu**

Abstract:

Nontyphoidal strains of *Salmonella enterica* are a major cause of foodborne illnesses and infection with these bacteria result in inflammatory gastroenteritis. Neutrophils are a dominant immune cell type found at the site of infection in *Salmonella*-infected individuals, but how they regulate infection outcome is not well understood. Here we used a co-culture model of primary human neutrophils and human intestinal organoids to probe the role of neutrophils during infection with two of the most prevalent *Salmonella* serovars: *Salmonella enterica* serovar Enteritidis and Typhimurium. Using a transcriptomics approach, we identified a dominant role for neutrophils in mounting differential immune responses including production of pro-inflammatory cytokines, chemokines, and antimicrobial peptides. We also identified specific gene sets that are induced by neutrophils in response to Enteritidis or Typhimurium infection. By comparing host responses to these serovars, we uncovered differential regulation of host metabolic pathways particularly induction of cholesterol biosynthetic pathways during Typhimurium infection and suppression of RNA metabolism during Enteritidis infection. Together these findings provide insight into the role of human neutrophils in modulating different host responses to pathogens that cause similar disease in humans.

Importance:

Nontyphoidal serovars of *Salmonella enterica* are known to induce robust neutrophil recruitment in the gut during early stages of infection, but the specific role of neutrophils in regulating infection outcome of different serovars is poorly understood. Due to differences in human infection progression compared to small animal models,

characterizing the role of neutrophils during infection has been challenging. Here we used a co-culture model of human intestinal organoids with human primary neutrophils to study the role of neutrophils during infection of human intestinal epithelium. Using a transcriptomics approach, we define neutrophil-dependent reprogramming of the host response to *Salmonella*, establishing a clear role in amplifying pro-inflammatory gene expression. Additionally, the host response driven by neutrophils differed between two similar nontyphoidal *Salmonella* serovars. These findings highlight the importance of building more physiological infection models to replicate human infection conditions to study host responses specific to individual pathogens.

Introduction:

Foodborne illnesses account for an estimated 48 million infections in the United States every year with 128,000 individuals needing to be hospitalized (1). One of the most common causes of foodborne disease is *Salmonella enterica,* which is responsible for an estimated 1.35 million infections in the United States each year (2). *Salmonella enterica* is comprised of over 2500 different serovars with *Salmonella enterica* serovar Typhimurium (STM) and Enteritidis (SE) among the most prevalent serovars globally. *Salmonella enterica* infects via the fecal-oral route and once it reaches the intestinal tract it stimulates a strong inflammatory response from the host leading to gastroenteritis and diarrheal disease (3). Although these symptoms are usually self-resolving, individuals with compromised immune systems or malnutrition can experience severe systemic, sometimes fatal, illness (4).

70 *Salmonella* pathogenesis is commonly studied *in vivo* using inbred mouse models.
71 Notably, disease progression caused by *Salmonella* is often different in mice compared
72 to humans, including the fact that mice rarely develop diarrhea during these infections
73 (5). To better understand human infection, human-derived cells including human intestinal
74 organoids (HIOs) have been used to define human-specific host responses to *Salmonella*
75 (6–8). HIOs are derived from human pluripotent stem cells and self-organize to form a 3-
76 dimensional polarized epithelium with differentiated epithelial cells and an underlying
77 mesenchyme (9). Bacteria, including *Salmonella,* are able to replicate and stimulate
78 robust inflammatory responses in HIOs (6–8, 10–12). Although the HIO model and other
79 tissue culture models have been invaluable in revealing human-specific responses to
80 *Salmonella* infection (6–8, 13–15), key features missing from these models are known to
81 shape the outcome of infection, including immune cells.
82
83 Several immune cell types contribute to the control and resolution of *Salmonella*
84 infections, however one of the earliest responders and the most abundant cell type found
85 in *Salmonella*-infected individuals are polymorphonuclear leukocytes (PMNs), specifically
86 neutrophils (16, 17). PMNs defend against bacterial infections through both cell-intrinsic
87 and -extrinsic mechanisms - antimicrobial effectors like degradative proteases and ion
88 chelators, production of reactive oxygen species and formation of sticky antimicrobial
89 neutrophil extracellular traps (NETs) can directly kill bacteria (18,19)). PMNs also can
90 influence surrounding cells and tissues, including the intestinal epithelium, changing the
91 microenvironment via molecular oxygen depletion, regulating nutrient availability, and
92 through production of inflammatory mediators (20, 21). How the interaction between

93 intestinal epithelial cells and PMNs affect the outcome of bacterial infections is still poorly
94 understood. To address this gap in knowledge, we generated a PMN-HIO model by co-
95 culturing primary human PMNs with HIOs that were infected with *Salmonella enterica*
96 serovar Enteritidis (SE) or Typhimurium (STM) by microinjection of bacteria into the
97 lumen. Using this PMN-HIO model, we characterized how PMNs modulate intestinal
98 epithelial host defenses during infection, compared to HIOs alone. We show here that the
99 presence of PMNs elevates intestinal epithelial proinflammatory signaling, including
100 production of cytokines, chemokines, and antimicrobial effectors. PMN-HIOs also
101 distinguished between the two serovars through differential upregulation of metabolic
102 pathways indicating that there are additional nuances in how PMN-HIOs respond to
103 different pathogens.
104
105 **Results:**
106 **PMNs enhance HIO immune activation and other transcriptional responses during**
107 ***Salmonella* infection**
108 PMNs are potent drivers of inflammation, so we reasoned that PMNs would likely
109 modulate the intestinal host response to *Salmonella* infection. Using the PMN-HIO model,
110 we previously characterized the degree of PMN recruitment and effect on bacterial
111 colonization during *Salmonella* infection (22). Here, to probe the contribution of PMNs to
112 the global intestinal transcriptional responses during infection, HIOs and PMN-HIOs were
113 microinjected with SE, STM or PBS and harvested at 8h post-infection (8hpi) for bulk
114 RNA-sequencing (RNA-seq). Principal component analysis (PCA) was performed on
115 normalized gene counts to determine whether PMNs drove separation between HIOs and

116 PMN-HIOs and therefore changed the transcriptional profile during infection (Fig. 1A).
117 While there was definitive segregation between infected HIOs in the presence and
118 absence of PMNs, there was no clear separation between PBS control HIOs and PMN-
119 HIOs, suggesting that PMNs change the transcriptional profile of the HIOs only during
120 infection. To determine which biological pathways contributed most to the segregation
121 between HIOs and PMN-HIOs, we extracted the loadings data from principal component
122 1 and subjected the top 50 genes to pathway enrichment analysis in Reactome to identify
123 biological processes that these genes participate in (Fig. 1B). Approximately 75% of these
124 genes belonged to the immune system, disease processes, and signal transduction
125 suggesting a dominant role of immune activation for PMNs in the PMN-HIO model.
126 Collectively, these data support that PMNs induce changes in HIO responses only during
127 infection and that PMNs primarily induce enrichment of immune-related pathways.
128
129 To further analyze which specific processes were induced by PMNs and how these
130 pathways were enriched under various culture conditions, we performed pathway
131 enrichment analysis of these top pathways with all genes that had a p-adjusted value
132 <0.05 relative to control PBS-injected HIOs (Fig. 1C, and Table S1). Each pathway was
133 analyzed for gene ratio (fraction of genes in a pathway that were significantly changed
134 relative to total genes in that pathway) plotted on the x-axis, and the statistical
135 significance, depicted as dot size, based on $-\log_{10}$(p-adjusted). As anticipated, immune
136 system-related pathways were among the most significantly enriched pathways in
137 response to infection (Fig. 1C). These included pathways belonging to processes
138 involving signaling by interleukins, Toll-like receptor signaling, as well as PMN-specific

139 pathways like neutrophil degranulation. We also detected enrichment of signal
140 transduction pathways that also relate to PMN function. These pathways were related to
141 Rho GTPase signaling. Activation of Rho GTPases has been shown in numerous studies
142 to be critical in membrane remodeling during *Salmonella* infection and are targeted by
143 secreted *Salmonella* effectors (23). Taken together, these results highlight the viability of
144 the PMN-HIO model, demonstrating that neutrophils enhance the inflammatory tone of
145 the HIO in an infection-specific manner.
146
147 One hallmark of infection with nontyphoidal *Salmonella* serovars is the development of
148 inflammatory diarrhea. Since many of the top genes driving segregation between PMN-
149 HIOs and HIOs were related to immune system processes, we assessed infected HIOs
150 and PMN-HIOs for enrichment of genes associated with diarrhea (24). As predicted, the
151 number of diarrhea-associated genes that were significantly changed increased with
152 infection (Fig 1D). Consistent with our findings that PMNs upregulate immune pathways,
153 the number of diarrhea-associated genes further increased in infected PMN-HIOs
154 compared to infected HIOs. PMNs also appeared to increase the fold change of many
155 genes that were changed in infected HIOs. These results suggest that PMNs not only
156 amplify inflammatory processes during intestinal infection but may also promote induction
157 of diarrhea.
158
159 To investigate how PMNs changed the HIO response during infection at the gene level,
160 significant gene changes were calculated relative to PBS control HIOs and filtered for
161 adjusted p-value <0.05 (Table S2). Venn diagrams were generated to compare gene

162 changes during SE infection +/- PMNs or STM infection +/-PMNs (Fig. 1E). Although a
163 substantial number of genes were changed during infection in both HIOs and PMN-HIOs,
164 over 1700 additional genes were induced in SE-infected PMN-HIOs and over 1900 in
165 STM-infected PMN-HIOs relative to HIOs alone. Importantly, there were very few genes
166 induced in PBS control PMN-HIOs, confirming that adding PMNs to the HIOs alone does
167 not trigger major changes in transcriptional programming, but the complex interaction
168 between PMNs, HIOs and *Salmonella* drove a robust transcriptional response. Together
169 these results demonstrate that co-culture with PMNs amplifies the HIO response to
170 *Salmonella* infection including expression of genes that were not induced in infected HIOs
171 alone, as well as enhanced enrichment of immune-related processes.

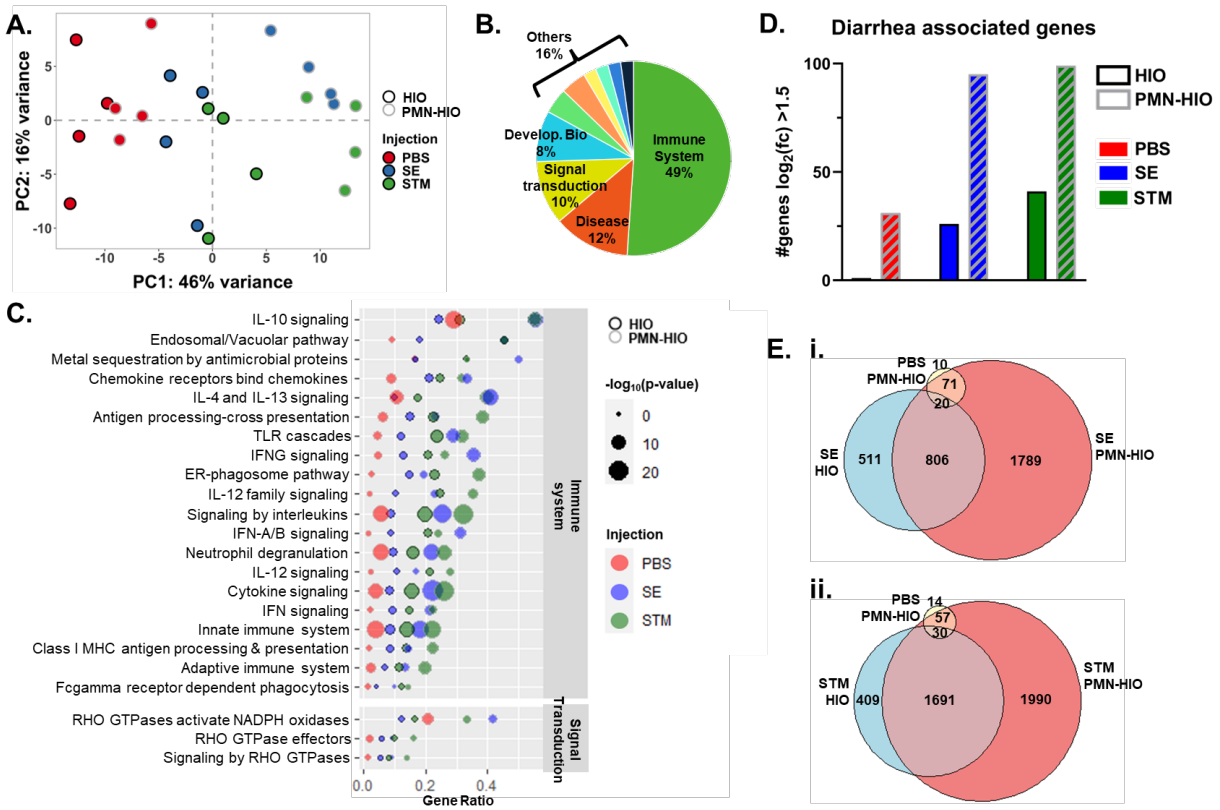

172

173 **Fig 1. PMNs enhance HIO immune activation and other transcriptional responses during**
174 ***Salmonella* infection**
175 A.PCA plot of HIOs and PMN-HIOs infected with STM or SE with PBS as the mock control for 8h.
176 B. Loadings data from PC1 was extracted from A to identify the top 50 genes driving separation

177 of samples via PC1. Genes were then assessed for pathway enrichment using the Reactome
178 database. Pie chart shows the percent of the top 50 pathways belonging to each of the Major
179 Reactome pathway categories C. Dot plot assessing pathway enrichment of the top 50 identified
180 pathways in (B) using all differentially expressed genes (p-adjusted value<0.05 compared to PBS-
181 injected HIOs). Gene ratio is shown on the x-axis and the dot size corresponds to the -log10(p-
182 value). HIO samples are outlined in black while PMN-HIOs are outlined in gray. PBS-injection
183 (red), SE-injection (blue), STM-injection (green). D. Number of diarrhea associated genes with p-
184 adjusted <0.05 and log2(fold change)>1.5 in each condition. Gene list for this analysis was used
185 from (23). E. Venn diagram comparing differentially regulated genes with p-adjusted value <0.05
186 relative to PBS-injected HIOs for SE-injected HIOs, PBS-injected PMN-HIOs, and SE-injected
187 PMN-HIOs (i.) and STM-injected HIOs, PBS-injected PMN-HIOs and STM-injected PMN-HIOs
188 (ii.).

189 **PMNs elevate production of cytokines and chemokines in the PMN-HIOs**

190 We recently reported that both SE and STM induce robust pro-inflammatory signaling in
191 the HIO through transcriptional upregulation of cytokine and chemokine genes and
192 downstream secretion of these effectors (6, 8). Because we observed a further increase
193 in pathway enrichment of several pro-inflammatory pathways in the infected PMN-HIOs
194 compared to infected HIOs, we examined the contribution of PMNs in changing
195 expression and production of some of these pro-inflammatory mediators including
196 cytokines and chemokines. Consistent with pathway enrichment results, PMN-HIOs
197 increased expression of almost every cytokine and chemokine that was significantly
198 changed during either SE or STM infection in the HIOs alone (Fig. 2A-2B). This elevated
199 PMN-dependent response was primarily driven by infection, as there was little
200 upregulation of these genes in PBS control PMN-HIOs. Of interest, in infected PMN-HIOs,
201 we observed increased transcript levels of cytokines CSF-3, IL-6, IL-8 (Fig. 2A) and
202 chemokines CXCL-10 and CCL-2 (Fig. 2B), all of which are essential for progression and
203 resolution of intestinal inflammation (25–27). To assess whether these transcriptional
204 changes were reflected at the protein level, supernatants from HIOs and PMN-HIOs were
205 collected for ELISA to measure cytokine and chemokine output (Fig. 2C). Protein level
206 analyses revealed similar patterns to the transcriptional results. Overall, the production of

207 most cytokines and chemokines in infected PMN-HIOs was increased compared to
208 infected HIOs or uninfected PMN-HIO controls. This included significant increases in IL-
209 6, IL-8, CXCL-10, and CCL-2 production in infected PMN-HIOs compared to infected
210 HIOs. However, some cytokines such as G-CSF (encoded by *CSF3*) or CXCL-2 did not
211 significantly change with the addition of PMNs. While most other pro-inflammatory
212 proteins correlated well with the transcript data, *CSF3* transcript was dramatically
213 upregulated in infected PMN-HIOs, compared to infected HIOs, even though there was
214 no difference in secreted protein levels. It is notable that although SE and STM induce
215 similar degrees of *CSF3* transcript upregulation, protein levels of G-CSF in the
216 supernatant are significantly lower in SE-infected PMN-HIOs compared to STM,
217 suggesting that SE may regulate G-CSF post-transcriptionally. All together, we found that
218 inflammatory signaling was elevated when PMNs are present in infected HIOs.

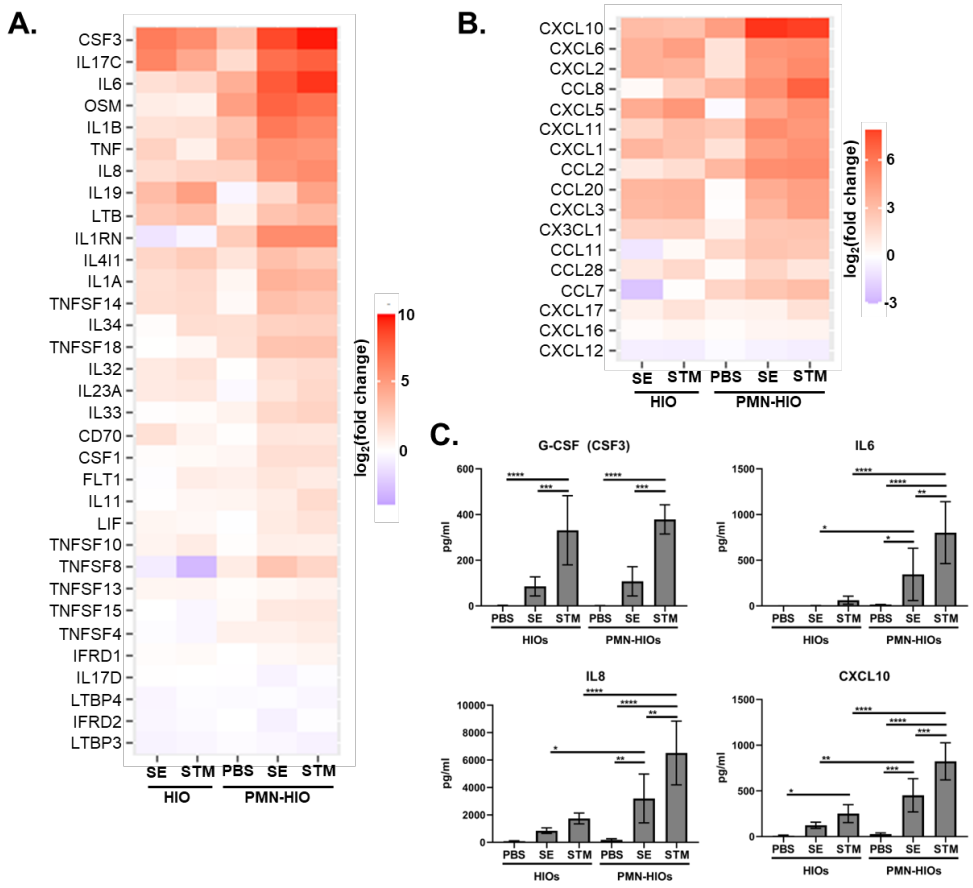

Fig 2. PMN-HIO co-culture amplifies production of cytokines and chemokines in infected HIOs

A-B. Gene expression data presented as log2(fold change) relative to PBS-injected HIOs for (A) cytokines and (B) chemokines. Genes that were significantly changed from PBS-injected HIOs in at least one condition with p-adjusted <0.05 are included. C. ELISA data from culture media sampled at 8hpi with 5 HIOs per well with n=4 replicates. Significance was determined by 2-way ANOVA where *p<0.05, **p<0.01, ***p<0.001, ****p<0.0001.

HIO co-culture with PMNs strengthens the antimicrobial environment

Antimicrobial effectors such as defensins are a key component of the host defense in the intestine and our previous work demonstrated that antimicrobial peptides (AMPs) are strongly upregulated during infection in the HIO model (6, 8). Among the pathways enriched (Fig. 1C), was ‘metal sequestration by antimicrobial proteins’ suggesting that PMNs strongly affect the antimicrobial milieu in the HIOs. PMNs are known to have a wide arsenal of antimicrobial effectors, but specifically how PMNs affect the antimicrobial

234 response during infection in complex environments such as in the PMN-HIO model has
235 not been fully defined. In contrast to what we had predicted, PMNs did not dramatically
236 enhance transcriptional upregulation of antimicrobial effectors above what was observed
237 in infected HIOs. This included beta-defensins (DEFB4A/B), nutritional immunity effectors
238 such as lipocalin (LCN2) or calprotectin (S100A8/9), and opsonins like SAA1/2 (Fig. 3A),
239 which were all highly upregulated during infection in both HIOs and PMN-HIOs. Since
240 PMNs represent approximately less than 5% of the cells in the PMN-HIO model (22), the
241 contribution of PMN transcripts in the overall bulk-RNA-seq is likely minimal. However,
242 analysis of culture supernatants via ELISA revealed that all these mediators were present
243 at significantly higher levels in infected PMN-HIOs compared to HIOs (Fig. 3B). Some of
244 these effectors were responsive to infection stimuli including beta-defensin (BD2,
245 encoded by DEFB4A and DEFB4B) and elafin (encoded by PI3) as they were not present
246 at high concentrations in the uninfected controls. In contrast, the nutritional immunity
247 effectors calprotectin and lipocalin were constitutively produced by PMNs, whether HIOs
248 were injected with PBS or *Salmonella*. Collectively, transcript and protein analyses of
249 infected PMN-HIOs reveal that a small population of neutrophils can substantially
250 enhance the antimicrobial environment.

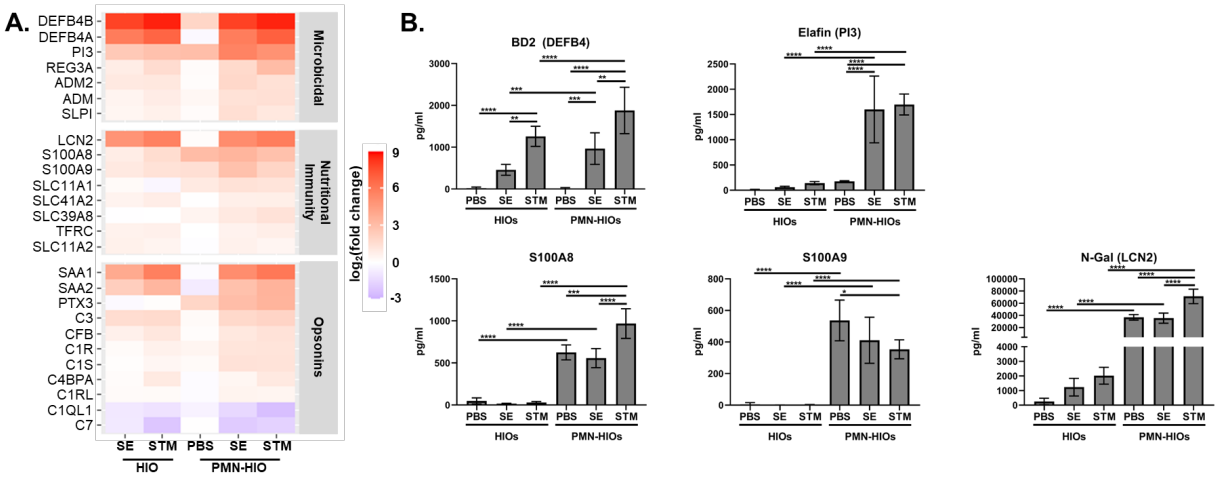

Fig 3. Presence of PMNs strengthens the antimicrobial environment
A. Gene expression data presented as log2(fold change) relative to PBS-injected HIOs for antimicrobial genes. Heatmap is divided into functional categories: Microbicidal, Nutritional Immunity, and Opsonins. Genes that were significantly changed from PBS-injected HIOs in at least one condition with p-adjusted <0.05 are included. B. ELISA data from culture media sampled at 8hpi with 5 HIOs per well with n=4 replicates. Significance was determined by 2-way ANOVA where *p<0.05, **p<0.01, ***p<0.001, ****p<0.0001.

PMN-HIOs induce unique responses to two nontyphoidal *Salmonella* serovars

SE and STM share high levels of gene homology but accessory genes unique to SE contribute to its pathogenesis in a mouse model of infection (28–30). We also found that these serovars elicit unique responses by human intestinal epithelium (8). Consistent with this earlier finding, we observed clustering of SE-infected PMN-HIOs away from STM-infected PMN-HIOs via principal component analysis (PC2) (Fig. 1A). These data suggest that PMN-HIOs also mount distinct responses to these two serovars. To characterize these responses, significant genes from SE, STM, and PBS-injected PMN-HIOs were compared to determine the overlap in transcriptional responses to infection (Fig. 4A). Surprisingly, while there was a core set of host genes that were changed in response to both SE and STM, the majority of genes were uniquely induced by only one serovar with over 1000 genes uniquely changed during SE-infection of the PMN-HIOs and over 2000 genes uniquely changed during STM-infection. To better characterize the functional

272 differences in these responses, the top 25 significant genes that were changed in either
273 SE-infected or STM-infected PMN-HIOs were plotted and assessed for fold change
274 relative to PBS-injected HIOs (Fig. 4B). The genes that were uniquely changed during
275 SE-infection belonged to multiple biological processes including metabolism (PFKFB4
276 and HK2) although RNA modification-related genes were highly represented among the
277 downregulated genes (ATIC, RRP12, NSUN2, and PUS1). More genes were
278 downregulated in SE-infected PMN-HIOs compared to STM-infected PMN-HIOs where
279 most genes that were uniquely responding to STM were upregulated. While these genes
280 also fell into multiple categories, upregulation of cholesterol biosynthetic genes in STM-
281 infected PMN-HIOs were highly prevalent in this heatmap (ACAT2, DHCR24, SCD,
282 ACLY, and LSS). To further characterize which pathways were differentially induced
283 during infection with the two serovars, pathway enrichment analysis on uniquely regulated
284 genes identified in Fig. 4A was performed. To classify these pathways into different
285 biological processes, each significantly enriched pathway was mapped back to the parent
286 pathway in the Reactome database (Fig. 4C, Tables S3 and S4). Out of the 1012 genes
287 that were uniquely induced in SE-infected PMN-HIOs, only 2 pathways were significantly
288 enriched: 'metabolism of RNA' and 'rRNA modification'. Most of the genes differentially
289 expressed only during SE infected were downregulated (Fig. 4B). In contrast, 143
290 Reactome pathways were enriched in STM-infected PMN-HIOs representing a much
291 more diverse set of biological processes. Cell cycle-related and signal transduction
292 pathways were all highly represented among genes that were only induced in STM-
293 infected PMN-HIOs, but we also noted that additional genes belonging to immune system
294 pathways were uniquely induced in STM-infected PMN-HIOs leading to higher

295 enrichment of these pathways. These findings suggest that while both serovars trigger
296 different responses by PMN-HIOs, responses unique to SE infection largely relate to RNA
297 metabolism while STM induces a broad range of host cell responses. Lastly, to compare
298 pathway enrichment across all differentially expressed genes, pathways that were
299 significant in either SE or STM infected PMN-HIOs were selected and sorted based on
300 biggest difference in gene ratio between the two serovars (Fig. 4D). Multiple biological
301 processes were differentially enriched when assessing the entire set of significant genes,
302 including cell cycle, disease-related processes specifically relating to beta-catenin
303 stability, immune system and metabolism related pathways. Pathways where SE
304 exhibited greater gene ratios compared to STM-infected samples were mostly related to
305 interferon signaling, although the 'HIF1A stabilization' pathway was also more enriched
306 in SE-infected PMN-HIOs. Most of these pathways were also highly enriched during STM-
307 infection with only a slight increase in gene ratio in the SE samples suggesting that both
308 serovars trigger these pathways. In contrast, STM infection resulted in much stronger
309 enrichment of beta-catenin related pathways and cholesterol biosynthesis pathways.
310 Sub-pathways of cholesterol biosynthesis, namely biosynthesis via lathosterol and
311 desmosterol had a gene ratio of 1 in STM-infected PMN-HIOs, meaning that all genes in
312 these pathways were significantly changed during infection. Overall, our findings reveal
313 differential responses between infection with SE and STM in the PMN-HIOs, including
314 regulation of genes involved in RNA modification in SE-infected PMN-HIOs. Host
315 responses to the two serovars were strikingly different in their stimulation of metabolic
316 pathways, specifically highly enriched cholesterol biosynthetic pathways observed only in
317 STM-infected PMN-HIOs.

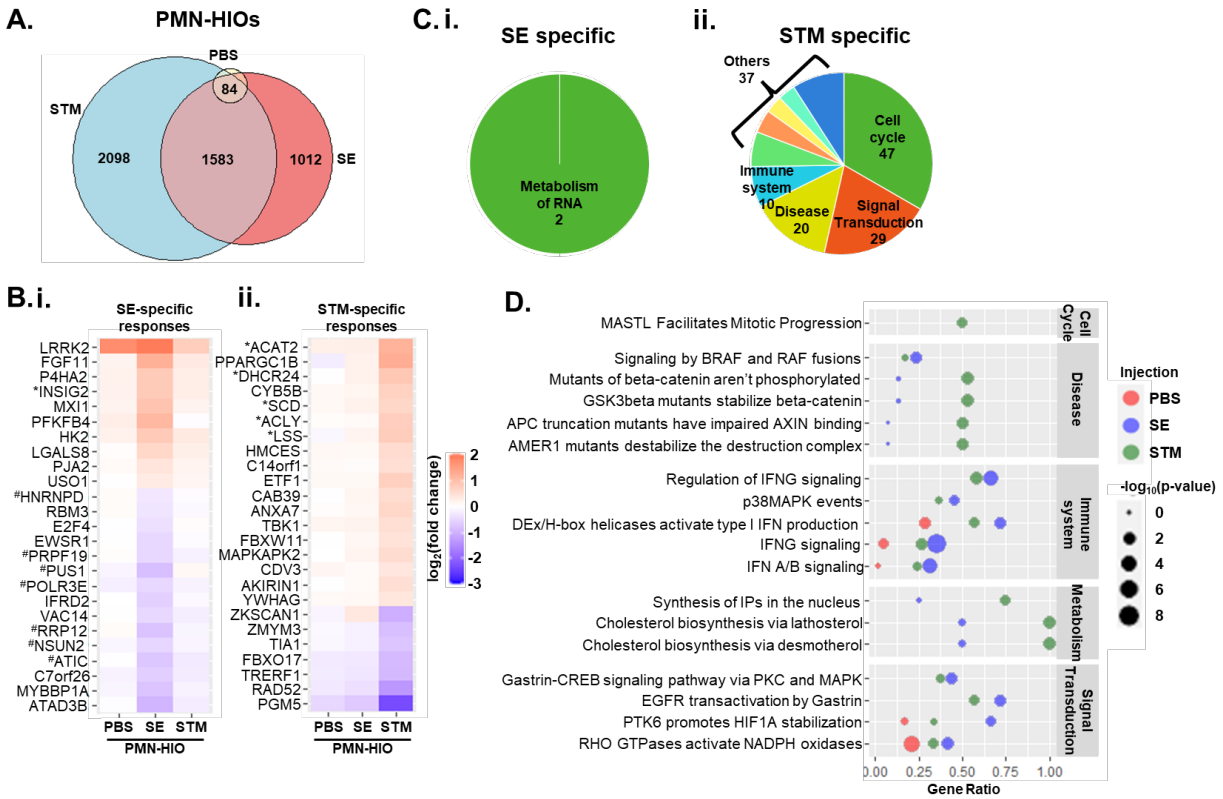

Fig 4. PMN-HIOs distinguish between SE and STM infection
A. Venn diagram comparing differentially regulated genes with p-adjusted value <0.05 relative to PBS-injected HIOs for STM-injected, SE-injected, or PBS-injected PMN-HIOs. B. Heatmap of unique differentially expressed genes. Top 25 genes based on adjusted p-value that were significant in only SE-injected PMN-HIOs (i.) or in STM-injected PMN-HIOs (ii.). Data are presented as log2(fold change) relative to PBS-injected HIOs. *Cholesterol biosynthetic genes, #RNA modification genes. C. Pathway enrichment analysis of 1012 SE-induced genes (i.) or 2098 STM-induced genes identified in (A) from the Reactome database. Pie chart shows the number of each major Reactome pathway category represented by the pathway enrichment results out of 2 significant pathways in SE-infected PMN-HIOs or 143 significant pathways in STM-infected PMN-HIOs. D. Dot plot assessing pathway enrichment in PMN-HIOs of all differentially expressed genes (p-adjusted value<0.05 compared to PBS-injected HIOs). Top pathways were selected by the biggest difference in gene ratio between SE and STM-injected PMN-HIOs. Gene ratio is shown on the x-axis and the dot size corresponds to the -log10(p-value). PBS-injection (red), SE-injection (blue), STM-injection (green).

Discussion:

PMNs, particularly neutrophils, are early responders to inflammation and represent a dominant immune cell type recruited to the intestine during infection with nontyphoidal *Salmonella* serovars. Although it is appreciated that neutrophils are present during the early phases of *Salmonella* infection, how neutrophils contribute to the host response in

339 a complex microenvironment like the intestine remains poorly understood. Here we used
340 a transcriptomics approach in a PMN-HIO co-culture model to probe the role of PMNs
341 during infection with two prevalent serovars of *Salmonella*: *Salmonella enterica* serovar
342 Enteritidis and Typhimurium. We identified a dominant role for PMNs in enhancing
343 inflammatory responses, including production of pro-inflammatory cytokines and
344 chemokines as well as antimicrobial proteins during infection with both serovars. More
345 broadly, PMNs acted on HIO cells to mount a more complex response to *Salmonella* as
346 there were over 1000 genes in each infection condition that were uniquely and
347 differentially expressed in the presence of PMNs. Lastly, we observed distinct responses
348 between serovars; metabolic pathways were differentially regulated in the PMN-HIOs
349 during SE and STM infection with robust enrichment of cholesterol biosynthesis genes
350 during infection with STM, and downregulation of RNA modification-related genes during
351 SE infection suggesting that PMNs can reprogram the environment in the presence of
352 different pathogens.
353
354 Infection with nontyphoidal strains of *Salmonella enterica* induce robust inflammatory
355 responses in the gut leading to gastroenteritis, and although neutrophils are known to be
356 present at the site of infection, the specific contribution in tuning the inflammatory
357 environment has been difficult to study in more complex animal models. We found via
358 RNA-seq, as well as assessing secreted effectors, that the presence of PMNs during
359 infection increased enrichment of cytokine signaling pathways, increased the
360 upregulation of several cytokines that were already induced in infected HIOs alone, as
361 well as led to a significant increase in levels of secreted cytokines and chemokines in the

362 culture supernatants. This pattern was also conserved for antimicrobial effectors including
363 a PMN-dependent upregulation in bactericidal and nutritional immunity related proteins.
364 While a subset of these effectors are likely produced by PMNs such as calprotectin
365 (encoded by S100A8/9) which is known to be highly produced in neutrophils, other
366 effectors such as beta-defensins (encoded by DEFB4A/B) or elafin (encoded by PI3) are
367 antimicrobial effectors known to be secreted by epithelial cells (31–33). This pattern would
368 suggest that PMNs program the epithelium to enhance antimicrobial responses during
369 infection. This pattern is supported by the prior finding that neutrophil elastase can induce
370 production of elafin by epithelial cells (34). We also note a dramatic increase in the
371 number of significant gene changes during infection in PMN-HIOs compared to HIOs,
372 suggesting that PMNs likely stimulate a broad epithelial response to infection given the
373 relatively low numbers of neutrophils in the PMN-HIOs. Further work may better elucidate
374 the specific contribution of each cell type in the response to infection by performing single-
375 cell RNA-seq, or other single cell approaches.
376
377 PMNs did not function to solely reprogram the inflammatory environment in response to
378 *Salmonella* infection, but also affected other cellular processes that differentiated
379 between infecting serovars. We found that over 3000 genes were differentially regulated
380 during infection with SE and STM in the PMN-HIO model. One of the most striking
381 differences we observed was transcriptional induction of cholesterol biosynthesis genes
382 in STM infection of the PMN-HIOs, but not SE infection. In contrast, we noted that SE-
383 infection uniquely induced upregulation of INSIG2, a negative regulator of cholesterol
384 biosynthesis. There are numerous reports investigating the role of cholesterol during

385 *Salmonella* infection including affecting invasion into epithelial cells, remodeling of the
386 *Salmonella* containing vacuole (SCV), bacterial replication, and susceptibility to typhoid
387 fever (35–43). Although there may be some cell type differences, the overarching pattern
388 from these studies reveal that increased cholesterol generally enhances *Salmonella*
389 infection. Our findings that SE does not induce upregulation of cholesterol biosynthetic
390 genes is intriguing. It is possible that the two serovars have evolved to have a different
391 dependence on cholesterol for productive infection. Alternatively, redistribution of existing
392 cholesterol in the cells may be sufficient for SE. We previously reported that SE and STM
393 exhibit different kinetics in their ability to invade and replicate within HIO epithelial cells,
394 with SE invading at reduced frequency compared to STM (8). Our findings here point to
395 cholesterol regulation as a potential mechanism that could contribute to differences in
396 infection kinetics. Differential regulation of cholesterol biosynthesis as well as other
397 serovar-specific responses warrant future study to better understand how these closely
398 related serovars may be interacting with the intestinal epithelium in distinct ways.
399
400 The findings reported herein lay the groundwork for many future directions. In addition to
401 PMN-dependent regulation of inflammatory responses and serovar-specific regulation of
402 cholesterol biosynthesis genes, we also measured a shift in gene expression in response
403 to *Salmonella* infection by using this co-culture model that was not observed in the HIO
404 model alone. This included an increase in expression of diarrhea-associated genes.
405 Modeling diarrheal diseases using mouse models has been difficult since mice rarely
406 develop diarrhea in response to bacterial infections. Thus, our results open up an area
407 for future study where the PMN-HIO co-culture model can be used to monitor human

408 genes that are associated with diarrheal responses when infected with *Salmonella* or
409 other microbial pathogens. Additionally, we show the feasibility of co-culturing HIOs with
410 immune cells and in the future, this will allow us to add back components incrementally
411 to model the intestinal environment and individually probe the role of immune cell
412 subtypes in various pathological conditions. Further characterization of the HIO model
413 and development of co-culture models of HIOs with immune cells will allow us to more
414 closely study mechanisms governing the complex human-specific responses of the
415 intestinal epithelium to bacterial infections.
416

417 **Acknowledgements**

418 This work was supported by the NIH awards U19AI116482-01 (V.B.Y, J.R.S, C.E.W, and
419 M.X.O) and R21AI13540 (M.X.O). A-L.E.L was supported by NIH T32 AI007528. We
420 thank the Host Microbiome Initiative, the Comprehensive Cancer Center Immunology
421 (supported by the NCI and NIH award P30CA046592) and Histology Cores and the DNA
422 Sequencing Core at University of Michigan Medical School. We gratefully acknowledge
423 the O'Riordan lab members for helpful discussions, and Dr. Roberto Cieza for assistance
424 with data management.
425

426 **Author contributions**

427 A-L.E.L and B.H.A performed the experiments and analyzed the data. A-L.E.L, M.X.O
428 and B.H.A designed the experiments and wrote the manuscript. R.P.B and D.R.H
429 assisted in RNA-seq analysis. S.H, V.K.Y, B.B and C.F assisted in HIO differentiation and

430 culturing. J.R.S, V.B.Y, C.E.W and J.S.K assisted in experimental preparation and data
431 interpretation.
432
433 **Declaration of interests**
434 The authors declare no competing interests.
435
436 **Materials and Methods:**
437 **Contact for reagent and resource sharing**
438 All RNA sequences are deposited in the EMBL-EBI Arrayexpress database (E-MTAB-
439 11089). Source code for RNA-seq analyses can be found at aelawren/PMN-HIO-RNA-
440 seq: R scripts for PMN-HIO RNA-seq analysis (github.com). Other reagents and
441 resources can be obtained by directing requests to the Lead Contacts, Basel Abuaita
442 (babuaita@lsu.edu) and Mary O'Riordan (oriordan@umich.edu).
443
444 **Experimental model and subject details**
445 **Human Intestinal Organoids (HIOs)**
446 HIOs were generated by the *In Vivo* Animal and Human Studies Core at the University of
447 Michigan Center for Gastrointestinal Research as previously described (9). Prior to
448 experiments, HIOs were removed from the Matrigel, washed with DMEM:F12 media, and
449 re-plated with 5 HIOs/well in 50µl of Matrigel (Corning) in ENR media ((DMEM:F12, 1X
450 B27 supplement, 2mM L-glutamine, 100ng/ml EGF, 100ng/ml Noggin, 500ng/ml
451 Rspondin1, and 15mM HEPES). Media was exchanged every 2-3 days for 7 days.
452

453 **Human Polymorphonuclear Leukocytes (PMNs)**

454 PMNs were isolated from blood of healthy human adult donors as previously described
455 (44), according to the protocol approved by the University of Michigan Medical School
456 (HUM00044257). Written consent was obtained from all donors. The purity of PMNs was
457 assessed by flow cytometry using APC anti-CD16 and FITC anti-CD15 antibodies
458 (Miltenyi Biotec), markers characteristic of human neutrophils.

459

460 **Bacterial Growth and HIO Microinjection**

461 *Salmonella enterica* serovar Typhimurium SL1344 (STM) and *Salmonella enterica*
462 serovar Enteritidis P125109 (SE) were used throughout the manuscript. Bacteria were
463 stored at -80°C in Luria-Bertani (LB, Fisher) medium containing 20% glycerol and cultured
464 on LB agar plates. Individual colonies were grown overnight at 37ºC under static
465 conditions in LB liquid broth. Bacteria were pelleted, washed and re-suspended in PBS.
466 Bacterial inoculum was estimated based on OD_{600} and verified by plating serial dilutions
467 on agar plates to determine colony forming units (CFU). Lumens of individual HIOs were
468 microinjected with glass caliber needles with 1µl of PBS, SE or STM (10^5 CFU/HIO) as
469 previously described (6, 45, 46). HIOs were then washed with PBS and incubated for 2h
470 at 37°C in ENR media. HIOs were treated with 100µg/ml gentamicin for 15 min to kill any
471 bacteria outside the HIOs, then incubated in fresh medium +/- PMNs (5 X 10^5
472 PMNs/5HIOs/well in a 24-well plate).

473

474 **Method Details**

475 **Cytokine Analyses**

476 For cytokine analysis, media from each well containing 5 HIOs/well were collected at 8hpi.
477 Cytokines, chemokines and antimicrobial proteins were quantified by ELISA at the
478 University of Michigan Cancer Center Immunology Core.
479
480 **RNA Sequencing and Analysis**
481 Total RNA was isolated from 5 HIOs per group with a total of 4 replicates per condition
482 using the mirVana miRNA Isolation Kit (Thermo Fisher). The quality of RNA was
483 confirmed, ensuring the RNA integrity number (RIN)> 8.5, using the Agilent TapeStation
484 system. cDNA libraries were prepared by the University of Michigan DNA Sequencing
485 Core using the TruSeq Stranded mRNA Kit (Illumina) according to the manufacturer's
486 protocol. Libraries were sequenced on Illumina HiSeq 2500 platforms (single-end, 50 bp
487 read length). All samples were sequenced at a depth of 10.5 million reads per sample or
488 greater. Sequencing generated FASTQ files of transcript reads that were pseudoaligned
489 to the human genome (GRCh38.p12) using kallisto software (47). Transcripts were
490 converted to estimated gene counts using the tximport package (48) with gene annotation
491 from Ensembl (49).
492
493 **Gene Expression and Pathway Enrichment Analysis**
494 Differential expression analysis was performed using the DESeq2 package (50) with *P*
495 values calculated by the Wald test and adjusted *P* values calculated using the Benjamani
496 & Hochberg method (51). Pathway analysis was performed using the Reactome pathway
497 database and pathway enrichment analysis in R using the ReactomePA software
498 package (52).

499

500 **Quantification and Statistical Methods**

501 RNA-seq data analysis was done using RStudio version 1.1.453. Plots were generated
502 using ggplot2 (53) with data manipulation done using dplyr (54). Euler diagrams of gene
503 changes were generated using the Eulerr package (55). Other data were analyzed using
504 Graphpad Prism 9. Statistical differences were determined using statistical tests indicated
505 in the fig. legends. The mean of at least 2 independent experiments were presented with
506 error bars showing standard deviation (SD). *P* values of less than 0.05 were considered
507 significant and designated by: *$P < 0.05$, **$P < 0.01$, ***$P < 0.001$ and **** $P < 0.0001$.

508

509 **Supplemental information**

510 **Table S1. Complete list of significant REACTOME pathways with p-value <0.05.**
511 Genes with p-adjusted value <0.05 and $\log_2$(fold change) >0 relative to PBS-injected
512 HIOs were selected for analysis.

513

514 **Table S2. Complete list of differentially expressed genes with p-adjusted value of**
515 **<0.05 compared to PBS-injected HIOs.**

516

517 **Table S3. Complete list of significant REACTOME pathways from genes**
518 **differentially expressed only in SE-infected PMN-HIOs.** Genes with p-adjusted value
519 <0.05, $\log_2$(fold change) >0 relative to PBS-injected HIOs and p-adjusted value >0.05 in
520 STM-infected PMN-HIOs were selected for analysis.

521

522 **Table S4. Complete list of significant REACTOME pathways from genes**
523 **differentially expressed only in STM-infected PMN-HIOs.** Genes with p-adjusted value
524 <0.05, $\log_2$(fold change) >0 relative to PBS-injected HIOs and p-adjusted value >0.05 in
525 SE-infected PMN-HIOs were selected for analysis.
526

527 **References**

528 1. CDC. 2020. Foodborne Germs and Illnesses.
529 https://www.cdc.gov/foodsafety/foodborne-germs.html. Retrieved 10 September
530 2021.

531 2. 2021. Salmonella Homepage. https://www.cdc.gov/salmonella/. Retrieved 10
532 September 2021.

533 3. Baird-Parker AC. 1990. Foodborne salmonellosis. Lancet 336:1231–1235.

534 4. Gilchrist JJ, MacLennan CA. 2019. Invasive Nontyphoidal Salmonella Disease in
535 Africa. EcoSal Plus 8.

536 5. Hapfelmeier S, Hardt W-D. 2005. A mouse model for S. typhimurium-induced
537 enterocolitis. Trends Microbiol 13:497–503.

538 6. Lawrence A-LE, Abuaita BH, Berger RP, Hill DR, Huang S, Yadagiri VK, Bons B,
539 Fields C, Wobus CE, Spence JR, Young VB, O'Riordan MX. 2021. Salmonella
540 enterica Serovar Typhimurium SPI-1 and SPI-2 Shape the Global Transcriptional
541 Landscape in a Human Intestinal Organoid Model System. MBio 12.

542 7. Forbester JL, Goulding D, Vallier L, Hannan N, Hale C, Pickard D, Mukhopadhyay
543 S, Dougan G. 2015. Interaction of Salmonella enterica Serovar Typhimurium with
544 Intestinal Organoids Derived from Human Induced Pluripotent Stem Cells. Infect
545 Immun 83:2926–2934.

546 8. Abuaita BH, Lawrence A-LE, Berger RP, Hill DR, Huang S, Yadagiri VK, Bons B,
547 Fields C, Wobus CE, Spence JR, Young VB, O'Riordan MX. 2021. Comparative
548 transcriptional profiling of the early host response to infection by typhoidal and non-
549 typhoidal Salmonella serovars in human intestinal organoids. PLoS Pathog
550 17:e1009987.

551 9. Spence JR, Mayhew CN, Rankin SA, Kuhar MF, Vallance JE, Tolle K, Hoskins EE,
552 Kalinichenko VV, Wells SI, Zorn AM, Shroyer NF, Wells JM. 2011. Directed
553 differentiation of human pluripotent stem cells into intestinal tissue in vitro. Nature
554 470:105–109.

555 10. Hill DR, Huang S, Nagy MS, Yadagiri VK, Fields C, Mukherjee D, Bons B, Dedhia
556 PH, Chin AM, Tsai Y-H, Thodla S, Schmidt TM, Walk S, Young VB, Spence JR. 2017.
557 Bacterial colonization stimulates a complex physiological response in the immature
558 human intestinal epithelium. Elife 6.

559 11. Karve SS, Pradhan S, Ward DV, Weiss AA. 2017. Intestinal organoids model human
560 responses to infection by commensal and Shiga toxin producing Escherichia coli.
561 PLoS One 12:e0178966.

562 12. Pradhan S, Weiss AA. 2020. Probiotic Properties of Escherichia coli Nissle in Human
563 Intestinal Organoids. MBio 11.

564 13. Schulte LN, Schweinlin M, Westermann AJ, Janga H, Santos SC, Appenzeller S,
565 Walles H, Vogel J, Metzger M. 2020. An Advanced Human Intestinal Coculture Model
566 Reveals Compartmentalized Host and Pathogen Strategies during Salmonella
567 Infection. MBio 11.

568 14. Hannemann S, Galán JE. 2017. Salmonella enterica serovar-specific transcriptional
569 reprogramming of infected cells. PLoS Pathog 13:e1006532.

570 15. Hannemann S, Gao B, Galán JE. 2013. Salmonella modulation of host cell gene
571 expression promotes its intracellular growth. PLoS Pathog 9:e1003668.

572 16. Rydström A, Wick MJ. 2007. Monocyte recruitment, activation, and function in the
573 gut-associated lymphoid tissue during oral Salmonella infection. J Immunol
574 178:5789–5801.

575 17. Tükel C, Raffatellu M, Chessa D, Wilson RP, Akçelik M, Bäumler AJ. 2006.
576 Neutrophil influx during non-typhoidal salmonellosis: who is in the driver's seat?
577 FEMS Immunol Med Microbiol 46:320–329.

578 18. Amulic B, Cazalet C, Hayes GL, Metzler KD, Zychlinsky A. 2012. Neutrophil function:
579 from mechanisms to disease. Annu Rev Immunol 30:459–489.

580 19. Brinkmann V, Reichard U, Goosmann C, Fauler B, Uhlemann Y, Weiss DS,
581 Weinrauch Y, Zychlinsky A. 2004. Neutrophil extracellular traps kill bacteria. Science
582 303:1532–1535.

583 20. Campbell EL, Bruyninckx WJ, Kelly CJ, Glover LE, McNamee EN, Bowers BE,
584 Bayless AJ, Scully M, Saeedi BJ, Golden-Mason L, Ehrentraut SF, Curtis VF,
585 Burgess A, Garvey JF, Sorensen A, Nemenoff R, Jedlicka P, Taylor CT, Kominsky
586 DJ, Colgan SP. 2014. Transmigrating neutrophils shape the mucosal
587 microenvironment through localized oxygen depletion to influence resolution of
588 inflammation. Immunity 40:66–77.

589 21. Fournier BM, Parkos CA. 2012. The role of neutrophils during intestinal inflammation.
590 Mucosal Immunol 5:354–366.

591 22. Lawrence A-LE, Berger RP, Hill DR, Huang S, Yadagiri VK, Bons B, Fields C, Sule
592 GJ, Knight JS, Wobus CE, Spence JR, Young VB, O'Riordan MX, Abuaita BH. 2022.
593 Human neutrophils direct epithelial cell extrusion to enhance intestinal epithelial host
594 defense during Salmonella infection. bioRxiv.

595 23. Patel JC, Galán JE. 2005. Manipulation of the host actin cytoskeleton by Salmonella-
596 -all in the name of entry. Curr Opin Microbiol 8:10–15.

597 24. Rouillard AD, Gundersen GW, Fernandez NF, Wang Z, Monteiro CD, McDermott
598 MG, Ma'ayan A. 2016. The harmonizome: a collection of processed datasets
599 gathered to serve and mine knowledge about genes and proteins. Database 2016.

600 25. Sumagin R, Parkos CA. 2015. Epithelial adhesion molecules and the regulation of
601 intestinal homeostasis during neutrophil transepithelial migration. Tissue Barriers
602 3:e969100.

603 26. Andrews C, McLean MH, Durum SK. 2018. Cytokine Tuning of Intestinal Epithelial
604 Function. Front Immunol 9:1270.

605 27. Wang D, Dubois RN, Richmond A. 2009. The role of chemokines in intestinal
606 inflammation and cancer. Curr Opin Pharmacol 9:688–696.

607 28. Ray S, Das S, Panda PK, Suar M. 2018. Identification of a new alanine racemase in
608 Salmonella Enteritidis and its contribution to pathogenesis. Gut Pathog 10:30.

609 29. Silva CA, Blondel CJ, Quezada CP, Porwollik S, Andrews-Polymenis HL, Toro CS,
610 Zaldívar M, Contreras I, McClelland M, Santiviago CA. 2012. Infection of mice by
611 Salmonella enterica serovar Enteritidis involves additional genes that are absent in
612 the genome of serovar Typhimurium. Infect Immun 80:839–849.

613 30. Dhanani AS, Block G, Dewar K, Forgetta V, Topp E, Beiko RG, Diarra MS. 2016.
614 Correction: Genomic Comparison of Non-Typhoidal Salmonella enterica Serovars
615 Typhimurium, Enteritidis, Heidelberg, Hadar and Kentucky Isolates from Broiler
616 Chickens. PLoS One 11:e0148706.

617 31. Caruso JA, Akli S, Pageon L, Hunt KK, Keyomarsi K. 2015. The serine protease
618 inhibitor elafin maintains normal growth control by opposing the mitogenic effects of
619 neutrophil elastase. Oncogene 34:3556–3567.

620 32. Pazgier M, Hoover DM, Yang D, Lu W, Lubkowski J. 2006. Human beta-defensins.
621 Cell Mol Life Sci 63:1294–1313.

622 33. Jukic A, Bakiri L, Wagner EF, Tilg H, Adolph TE. 2021. Calprotectin: from biomarker
623 to biological function. Gut 70:1978–1988.

624 34. Reid PT, Marsden ME, Cunningham GA, Haslett C, Sallenave JM. 1999. Human
625 neutrophil elastase regulates the expression and secretion of elafin (elastase-
626 specific inhibitor) in type II alveolar epithelial cells. FEBS Lett 457:33–37.

627 35. Santos AJM, Meinecke M, Fessler MB, Holden DW, Boucrot E. 2013. Preferential
628 invasion of mitotic cells by Salmonella reveals that cell surface cholesterol is maximal
629 during metaphase. J Cell Sci 126:2990–2996.

630 36. Misselwitz B, Dilling S, Vonaesch P, Sacher R, Snijder B, Schlumberger M, Rout S,
631 Stark M, von Mering C, Pelkmans L, Hardt W-D. 2011. RNAi screen of Salmonella
632 invasion shows role of COPI in membrane targeting of cholesterol and Cdc42. Mol
633 Syst Biol 7:474.

634 37. Nawabi P, Catron DM, Haldar K. 2008. Esterification of cholesterol by a type III
635 secretion effector during intracellular Salmonella infection. Mol Microbiol 68:173–
636 185.

637 38. Greene AR, Owen KA, Casanova JE. 2021. Salmonella Typhimurium manipulates
638 macrophage cholesterol homeostasis through the SseJ-mediated suppression of the
639 host cholesterol transport protein ABCA1. Cell Microbiol 23:e13329.

640 39. Catron DM, Lange Y, Borensztajn J, Sylvester MD, Jones BD, Haldar K. 2004.
641 Salmonella enterica serovar Typhimurium requires nonsterol precursors of the
642 cholesterol biosynthetic pathway for intracellular proliferation. Infect Immun 72:1036–
643 1042.

644 40. Gilk SD, Cockrell DC, Luterbach C, Hansen B, Knodler LA, Ibarra JA, Steele-
645 Mortimer O, Heinzen RA. 2013. Bacterial colonization of host cells in the absence of
646 cholesterol. PLoS Pathog 9:e1003107.

647 41. Rotimi SO, Ojo DA, Talabi OA, Balogun EA, Ademuyiwa O. 2012. Tissue
648 dyslipidemia in Salmonella-infected rats treated with amoxillin and pefloxacin. Lipids
649 Health Dis 11:152.

650 42. Huang F-C. 2014. The critical role of membrane cholesterol in salmonella-induced
651 autophagy in intestinal epithelial cells. Int J Mol Sci 15:12558–12572.

652 43. Alvarez MI, Glover LC, Luo P, Wang L, Theusch E, Oehlers SH, Walton EM, Tram
653 TTB, Kuang Y-L, Rotter JI, McClean CM, Chinh NT, Medina MW, Tobin DM, Dunstan
654 SJ, Ko DC. 2017. Human genetic variation in *VAC14* regulates *Salmonella* invasion
655 and typhoid fever through modulation of cholesterol. Proc Natl Acad Sci U S A
656 114:E7746–E7755.

657 44. Abuaita BH, Sule GJ, Schultz TL, Gao F, Knight JS, O'Riordan MX. 2021. The IRE1α
658 Stress Signaling Axis Is a Key Regulator of Neutrophil Antimicrobial Effector
659 Function. J Immunol https://doi.org/10.4049/jimmunol.2001321.

660 45. Abuaita BH, Lawrence A-LE, Berger RP, Hill DR, Huang S, Yadagiri VK, Bons B,
661 Fields C, Wobus CE, Spence JR, Young VB, O'Riordan MX. 2020. Comparative
662 transcriptional profiling of the early host response to infection by typhoidal and non-
663 typhoidal Salmonella serovars in human intestinal organoids. bioRxiv.

664 46. Hill DR, Huang S, Tsai Y-H, Spence JR, Young VB. 2017. Real-time Measurement
665 of Epithelial Barrier Permeability in Human Intestinal Organoids. J Vis Exp
666 https://doi.org/10.3791/56960.

667 47. Bray NL, Pimentel H, Melsted P, Pachter L. 2016. Near-optimal probabilistic RNA-
668 seq quantification. Nat Biotechnol 34:525–527.

669 48. Soneson C, Love MI, Robinson MD. 2015. Differential analyses for RNA-seq:
670 transcript-level estimates improve gene-level inferences. F1000Res 4:1521.

671 49. Rainer J. 2017. EnsDb.Hsapiens.v75: Ensembl based annotation package. R
672 package version 2.99.0.

673 50. Love MI, Huber W, Anders S. 2014. Moderated estimation of fold change and
674 dispersion for RNA-seq data with DESeq2. Genome Biol 15:550.

675 51. Benjamini Y, Hochberg Y. 1995. Controlling the False Discovery Rate: A Practical
676 and Powerful Approach to Multiple Testing. Journal of the Royal Statistical Society:
677 Series B (Methodological) https://doi.org/10.1111/j.2517-6161.1995.tb02031.x.

678 52. Yu G, He Q-Y. 2016. ReactomePA: an R/Bioconductor package for reactome
679 pathway analysis and visualization. Mol Biosyst 12:477–479.

53. Wickham H. 2016. ggplot2: Elegant Graphics for Data Analysis. Springer.

54. Wickham H, Francois R, Henry L, Müller K, Others. 2015. dplyr: A grammar of data manipulation. R package version 0 4 3.

55. Larsson J. 2019. eulerr: Area-Proportional Euler and Venn Diagrams with Ellipses (R package version 5.1.0).